Journal of Systematic Palaeontology **2** (4): 269–284
DOI: 10.1017/S147720190400149X Printed in the United Kingdom
Issued 26 January 2005

A new early Devonian Trigonotarbid Arachnid from the Windyfield chert, Rhynie, Scotland

Stephen R. Fayers
Department of Geology and Petroleum Geology, Meston Building, King's College, University of Aberdeen, Aberdeen, AB24 3UE, UK

Jason A. Dunlop
Institut für Systematische Zoologie, Museum für Naturkunde der Humboldt-Universität zu Berlin, Invalidenstrasse 43, D-10115 Berlin, Germany

Nigel H. Trewin
Department of Geology and Petroleum Geology, Meston Building, King's College, University of Aberdeen, Aberdeen, AB24 3UE, UK

SYNOPSIS A new, exceptionally preserved, trigonotarbid (Arachnida, Trigonotarbida, Palaeocharinidae), *Palaeocharinus tuberculatus* sp. nov. is described from the early Devonian (Pragian) Windyfield chert of Rhynie, Aberdeenshire, Scotland, UK. The specimens found are almost twice the size of previous Rhynie palaeocharinids and display an autapomorphic, microtuberculate ornament over the whole body. This tuberculation and possible developing tergite and sternite divisions, which the microtubercles in places appear to define, show significant similarities with the possibly closely related Carboniferous family Anthracomartidae.

KEY WORDS Palaeocharinidae, *Palaeocharinus*, Pragian, terrestrial, hot springs

Contents

Introduction **269**
Geological background and setting **270**
Material and methods **270**
Occurrence and taphonomy **271**
Systematic palaeontology **271**
TETRAPULMONATA Shultz, 1990 271
Order TRIGONOTARBIDA Petrunkevitch, 1949 271
Family PALAEOCHARINIDAE Hirst, 1923 271
Genus *PALAEOCHARINUS* Hirst, 1923 271
Palaeocharinus tuberculatus sp. nov. 272
General description **272**
Dorsal prosoma 272
Ventral prosoma 275
Opisthosoma 276
Appendages 279
Discussion **281**
Acknowledgments **283**
References **283**

Introduction

Trigonotarbids are an extinct arachnid order and are the most basal members of the so-called Tetrapulmonata clade (Shear *et al.* 1987; Shear 2000), which also includes spiders, Amblypygi (whip spiders) and Uropygi (whip scorpions). Although superficially similar to spiders, trigonotarbids are distinguished by the absence of silk-producing spinnerets and the possession of a segmented opisthosoma in which most of the tergites are divided longitudinally into three or five sclerites, comprising a broad median plate flanked by two or four narrower lateral plates. The oldest trigonotarbid,

Published online 09 Mar 2010

Palaeotarbus jerami (Dunlop 1996*a*), comes from the late Silurian (Přídolí) of Ludford Lane, and the order extends to the early Permian (Rößler *et al.* 2003), attaining its highest diversity in genera and species in the late Carboniferous. Trigonotarbids were probably an important terrestrial faunal element during the mid–late Palaeozoic (e.g. Rolfe 1980).

The early Devonian trigonotarbids from the Rhynie cherts are perhaps the best known members of the group in terms of morphology. As with other elements of the chert biota, preservation is often exquisite with both exuviae and individuals being commonly preserved in remarkable, three-dimensional anatomical detail. Specimens can be so well preserved that features such as their book lungs (Claridge & Lyon 1961), mouthparts (Dunlop 1994*a*) and even muscle tendons (Dunlop 1994*b*) have been identified. The currently known trigonotarbids from Rhynie – all belonging to the family Palaeocharinidae – have only been described from the Rhynie chert (Hirst 1923; Dunlop 1994*b*). During recent studies on a new, adjacent site, the Windyfield chert (Trewin & Rice 1992; Fayers 2003), a number of trigonotarbids have been found. Most common were the previously described species of *Palaeocharinus* (Hirst 1923), but two new, larger forms have also been discovered – one of which is described herein as a new species.

Geological background and setting

The Rhynie and Windyfield cherts found at Rhynie, Aberdeenshire, Scotland (Fig. 1), both occurring in the Dryden Flags Formation (Rice *et al.* 2002), represent the surface expression of a metaliferous hydrothermal system that was active in the Rhynie area during the early Devonian (Pragian: Rice *et al.* 1995, 2002). The cherts are renowned for their exceptionally well preserved terrestrial and freshwater biota. Many of the land plants preserved have proved to be of fundamental significance in palaeobotany (Cleal & Thomas 1995), while the arthropods represent the most diverse fauna of associated terrestrial and freshwater fossils from strata of a comparable age anywhere in the world (Anderson & Trewin 2003).

The Windyfield chert, located approximately 700 m to the north-east of the Rhynie chert locality (Fig. 1), is slightly higher in the stratigraphic succession than the latter and comprises laterally discontinuous lenticular, pod-like bodies of chert interbedded with hydrothermally altered shales and sandstones (Rice *et al.* 2002). The chert morphologies, the enclosed biota and their taphonomy are broadly comparable to the Rhynie chert (Trewin 1994, 1996), but the Windyfield cherts tend to exhibit greater degrees of brecciation (Fayers 2003). At the Windyfield locality, a loose chert block displaying a geyserite splash texture is the only physical evidence, so far, for contemporaneous geyser activity in the area (Trewin 1994).

The background setting was an alluvial plain set in a narrow half-graben basin with mainly overbank deposition on floodplains and in ephemeral lakes, with occasional sheetflood events sourced from the axial river system and basin margins (Trewin 1994, 2001). The cherts were deposited as subaerial siliceous sinters, although some beds represent the silicified contents of freshwater pools (Anderson & Trewin 2003; Trewin *et al.* 2003). The Windyfield chert represents

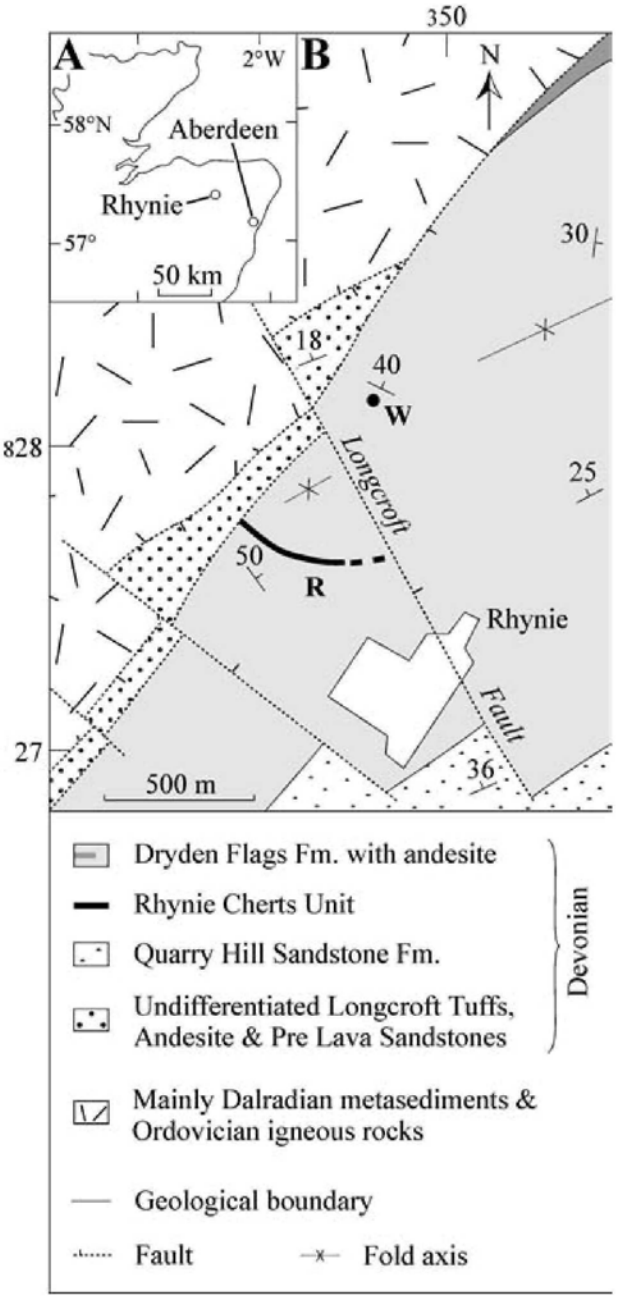

Figure 1 **A,** Map of north-east Scotland showing the location of Rhynie. **B,** Simplified geological map of the area north of Rhynie village showing the location of the Windyfield chert (W) and the known extent of the Rhynie chert subcrop (R). Modified from Rice *et al.* (2002).

an area of deposition proximal to hot spring activity given the presence of a geyser vent rim, a high degree of chert brecciation and hydrothermal alteration of the interbedded sediments (Fayers 2003). The Rhynie cherts, however, primarily represent sinter deposition on the distal reaches of an outwash apron from hot springs (Trewin & Wilson 2004).

Material and methods

The chert containing the new trigonotarbid was recovered from an *in situ* 'pod' excavated during a programme of

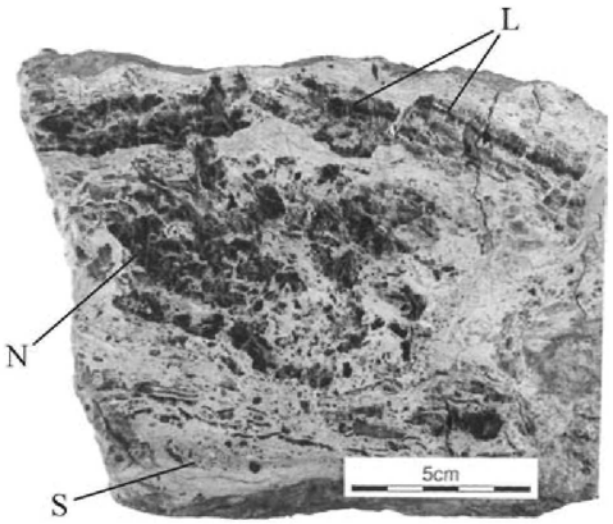

Figure 2 Vertical section through a block of brecciated Windyfield chert recovered from the *in situ* 'pod' discovered in trench T3 described by Anderson & Trewin (2003). L, microbially laminated chert; N, nodular chert; S, chert-cemented sandstone.

trenching in the vicinity of Windyfield farm during the summer of 1997 (trench T3 of Anderson & Trewin 2003: text-figs 1B & 2). For details of the trenching, stratigraphy and sedimentology of the chert-bearing sequence see Rice *et al.* (2002) and Fayers (2003).

Specimens were discovered by examining cut slices of chert under a binocular microscope. Samples found to contain diagnostic material were trimmed to an appropriate size and then mounted on glass thin section slides using thermoplastic cement. They were then gradually lapped until other diagnostic assemblages of cuticle were exposed or until the chert was of a thickness allowing examination under the microscope using transmitted light. For further details of chert preparation procedures see Anderson & Trewin (2003).

Photomicrographs of the material were taken using a combination of transmitted and reflected light. *Camera lucida* drawings of the fossil material proved particularly useful in resolving taxonomic features that could not always be adequately photographed given the three-dimensional nature of the preservation in the chert. The material has been deposited in the Type and Figured collections of the Department of Geology and Petroleum Geology, University of Aberdeen, UK (AUGD).

Occurrence and taphonomy

The *in situ* 'pod' comprises more or less autochthonous fragments of bluish black, microbially laminated chert and internally massive nodular chert, set within a matrix of silicified sandstone (Fig. 2). Internally, the nodular chert displays filamentous, coprolitic and clotted microscopic textures (*sensu* Anderson & Trewin 2003) and a mixed terrestrial and freshwater biota, indicating silicification of the organic contents of a small freshwater pool (Fayers 2003; Trewin *et al.* 2003). The laminated cherts comprise stacked microbial laminae interspersed with chert-cemented fenestrae. Microbial filaments often exhibit phototactic orientations and, as such, probably represent photosynthetic bacteria. The laminated cherts are interpreted as representing silicified microbial mats that were growing at the pool margins, possibly extending as floating mats across the pool surface (Fayers 2003).

The specimens of the new trigonotarbid occur in both the laminated and nodular cherts, ranging from near complete animals to scattered podomeres and fragments of cuticle. The most complete and best preserved specimens have been found in the laminated cherts (Fig. 2), which occasionally possess a colour and transparency similar to amber. It is by no means certain whether the specimens represent dead individuals or exuviae, since internal structures such as book lungs have not been observed. After moulting, an arachnid's carapace tends to end up somewhat disarticulated from the legs, thus the more complete specimens are probably the remains of individuals.

Although many of the specimens have been found in cherts showing fabrics and a biota indicative of an aquatic environment, these trigonotarbids were almost certainly terrestrial predators. Their inclusion in deposits of an aquatic setting, together with other terrestrial taxa, is most probably due either to the flooding of their normal environment by hot spring fluids or they were perhaps washed into existing pools of water. The association of the microbially laminated cherts with these nodular cherts of aquatic origin could suggest that some of these trigonotarbids were occasionally living and hunting on floating microbial mats. In modern hot spring environments, wolf spiders (Lycosidae) have been observed to hunt over the surfaces of microbial mats on sinter aprons (e.g. Brock 1994), and also on mats floating on the surfaces of pools that are thick and cohesive enough to support the weight of small invertebrates (pers. obs.).

Systematic palaeontology

TETRAPULMONATA Shultz, 1990
Order **TRIGONOTARBIDA** Petrunkevitch, 1949
Family **PALAEOCHARINIDAE** Hirst, 1923
Genus ***PALAEOCHARINUS*** Hirst, 1923

TYPE SPECIES. *Palaeocharinus rhyniensis* Hirst, 1923, designated by Petrunkevitch (1949: 237). Other included species: *P. scourfieldi* Hirst, 1923, *P. calmani* Hirst, 1923, *P. kidstoni* Hirst, 1923, *P. hornei* (Hirst, 1923) and *P. tuberculatus* sp. nov.

DIAGNOSIS. Palaeocharinids with anterior median lobe of the clypeus forming a pair of prominent, projecting acute processes. The processes are the distal derivatives of two subparallel ridges that extend from the level of the median eyes to the anterior margin of the carapace (after Shear *et al.* 1987).

OCCURRENCE. Early Devonian (Pragian) of Rhynie, Aberdeenshire, Scotland.

REMARKS. Hirst (1923) originally described five species from the Rhynie chert under two genera: *Palaeocharinus* (four species) and *Palaeocharinoides* (one species). Genera were based on the posterior margin of the sternum: a straight versus an acute margin, respectively. Shear *et al.* (1987) rejected this as a generic character and synonymised *Palaeocharinoides* with *Palaeocharinus*. Provisional studies

of Hirst's types (Dunlop 1994*b*) suggests that at least some of his species are based on features caused by postmortem alteration associated with a supposedly diagnostic row of teeth on the chelicerae and/or the angle at which the carapace could be seen in the matrix. A formal revision is planned and we suspect only two of Hirst's original five species may be valid.

The new trigonotarbid described here can be referred with some confidence to *Palaeocharinus*. It has the characteristic box-shaped carapace with a projecting, toothed clypeus bearing two longitudinal subparallel ridges; lateral eye tubercles with major and minor eye lenses (probably a plesiomorphy); and an undivided ninth tergite, which is almost as wide as the opisthosoma. Its body length (over 5 mm) and its microtuberculate abdominal tergites are consistent with the diagnosis given for the Upper Devonian (late Famennian) palaeocharinid genus *Gigantocharinus* Shear, 2000. However, in detail the new Rhynie fossils are far more reminiscent of *Palaeocharinus*. In particular, the position of the eye tubercles and disposition of the lateral eye lenses is practically identical to that seen in other *Palaeocharinus* material (see Shear *et al.* 1987: fig. 6). Lateral eye tubercles are equivocal in *Gigantocharinus*. Unlike *Gigantocharinus*, the carapace of our new material lacks a rebordered posterior margin and, although it posesses a series of distinct pits (see below), it lacks the clearly lobate carapace seen in *Gigantocharinus*, which is more reminiscent of Carboniferous families such as Aphantomartidae (see Rößler *et al.* 2003). In all the Rhynie fossils the ninth tergite is broad and almost the full width of the opisthosoma. In *Gigantocharinus*, in contrast, the ninth tergite is narrow and for most of its length is flanked by the eighth tergite (Shear 2000). Indeed, in the original description, even Shear raised doubts about the assignment of *Gigantocharinus* to Palaeocharinidae.

Palaeocharinus tuberculatus sp. nov. (Figs 3–10)

ETYMOLOGY. The specific epithet is in reference to the distinctive tuberculate ornament of the animal.

TYPE MATERIAL. Holotype: Aberdeen University, Geology Department, AUGD12409 from the early Devonian (Pragian) Windyfield Chert, Rhynie, Aberdeenshire, Scotland, UK. Nearly complete specimen with articulated appendages. Four paratypes, from the same locality, designated AUGD12410–3.

DIAGNOSIS. Palaeocharinid with near symmetrical arrangement of microtubercles on the carapace forming a pattern of distinct polygonal and circular pits. Walking legs and pedipalps with regular longitudinal rows of microtubercles. Regular ornament of microtubercles on the dorsum of the opisthosoma and fringing the lateral margin.

GENERAL DESCRIPTION

Two nearly complete specimens have been discovered (AUGD12409 and AUGD12412). The former occurs in very clear chert containing bacterial filaments, is very well preserved and morphological details are exceptionally clear (Figs 3A & 4). In comparison, AUGD12412, which occurs on the edge of a chert sample, is slightly fragmented and many details are obscured by organic inclusions and detrital grains. Much of the prosoma of the latter has been lost during the thin sectioning process, but most of the opisthosoma and legs are present. AUGD12413 comprises the left side of a prosoma with three partial leg appendages. The other paratypes are near complete individuals, discovered in sequential chert slices, such that AUGD12410 contains a tarsus and isolated claws from the same animal in AUGD12409 and AUGD12411 contains articulated legs belonging to the same animal in AUGD12412.

The body of the holotype (Figs 3–5) is approximately 6 mm in length: prosoma 2.2 mm, opisthosoma *c.* 3.8 mm. All cuticle shows the same reticulate sculpture observed in previous *Palaeocharinus* species.

Dorsal prosoma

The prosomal dorsal shield or carapace is box-shaped, up to 2 mm wide and tapers towards the anterior end into a sharply projecting clypeus (Figs 3, 6A & 6B). This bears two subparallel ridges of spine-like projections on its anterior surface (Fig. 6A). These begin in front of the median eye tubercle (see below) and terminate in two spines at the anterior end of the clypeus. A further pair of spines occurs ventral and slightly posteriolaterally to these terminal spines (Figs 5 & 6A).

Immediately behind the clypeus is the median eye tubercle (Fig. 3B). A pair of median eye lenses is present, although difficult to resolve due to the faintness of the cuticle and depth within the holotype specimen (Figs 3B & 7). The eye lenses are separated medially by a distinct line of microtubercles, forming part of the characteristic ornament of this animal (see below). Laterally, and just behind the median eye tubercle are a pair of lateral eye tubercles (Figs 3B, 6 & 7). The lateral eye tubercles exhibit an ornament typical of the rest of the carapace, comprising a series of smaller, dark microtubercles. These are arranged as two subparallel rows beginning behind and slightly medially of the eye tubercle and running across the anterior surface, the size of the microtubercle increasing anteriorly (Figs 3B, 6B, 6C & 7B). The lateral eye tubercles bear a series of major and minor eye lenses that are practically identical to those seen in other *Palaeocharinus* material (see Shear *et al.* 1987: fig. 6). Most clearly seen on the holotype, these comprise a staggered row of up to 10 minor eye lenses separating a lower, anterior lateral lens from an upper, posterior median eye lens and a posterior lateral lens (Figs 6C & 7B).

The posterior margin of the carapace is broadly and shallowly excavated (Fig. 3). The lateral margins each comprise five scalloped indentations accommodating the coxa–trochanter articulations of the legs and pedipalps. The lateral border of the carapace, above the indentations and towards the clypeus, is strongly rebordered (Figs 6A & 7A).

The carapace exhibits a very distinctive, autapomorphic microtuberculate ornament. The tuberculation is nearly symmetrical about the carapace midline. It comprises a series of large and small microtubercles forming circles and polygons across the entire cuticle surface (Figs 3, 6 & 7). Each line of microtubercles forms a slight to occasionally pronounced ridge, so that the centres of the polygons or circles form depressions, giving the carapace a pitted appearance. Anteriorly, the tuberculation forms a medial ridge between the median eye lenses (see above), which then bifurcates and passes into the pair of spiny ridges on the front of the clypeus (Figs 3B, 6A, 6B & 7). On the dorsal surface, the

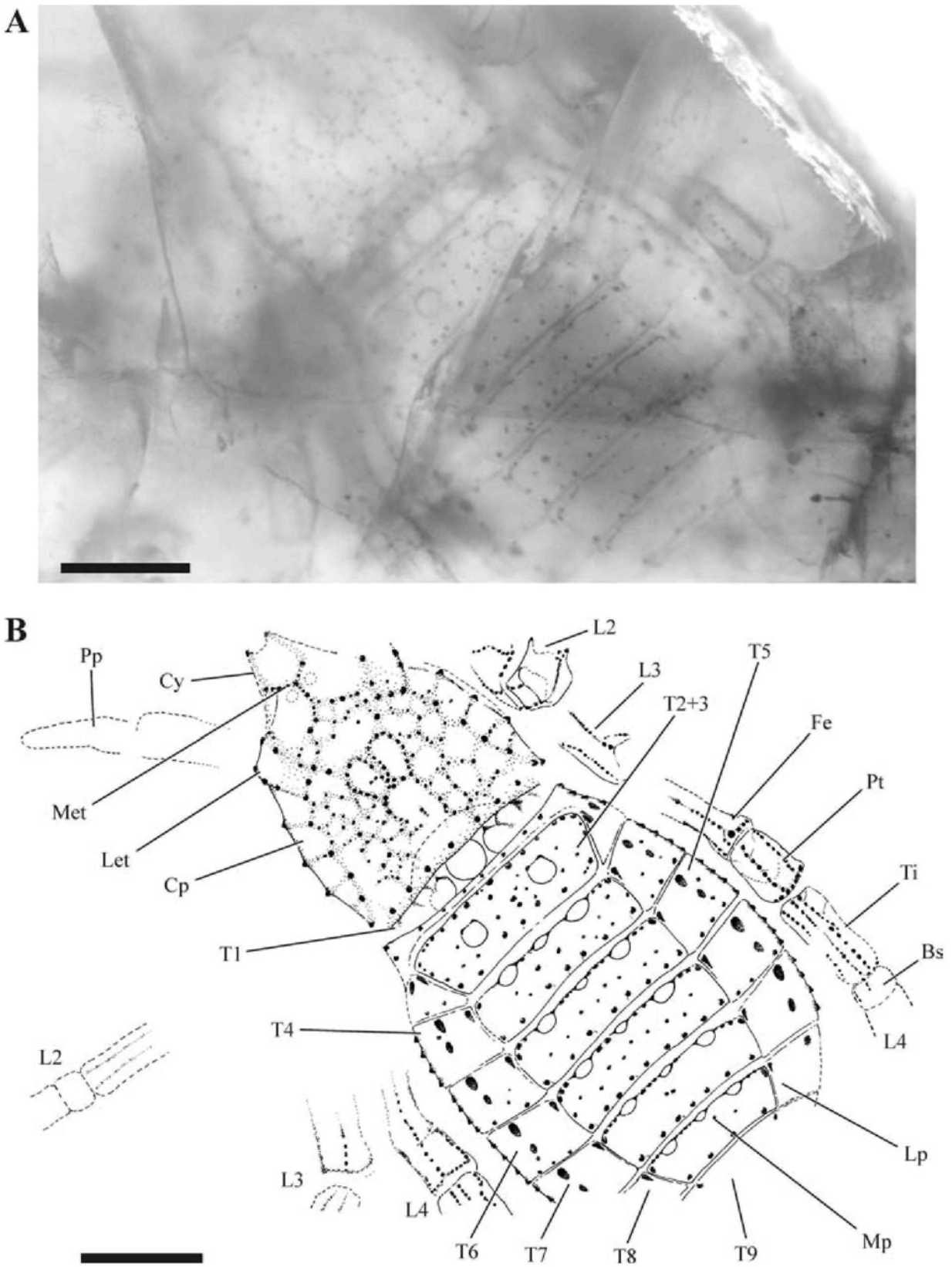

Figure 3 *Palaeocharinus tuberculatus* sp. nov., Pragian, Rhynie, Scotland. AUGD12409. **A**, Dorsal view of the holotype. A near complete specimen in remarkably clear, microbially laminated chert. Scale bar = 1 mm. **B**, *Camera lucida* drawing of the holotype showing the dorsal anatomy and ornamentation. Bs, basitarsus; Cy, clypeus; Cp, carapace; Fe, femur; L, walking legs (numbered); Let, lateral eye tubercle; Lp, lateral plate; Met, median eye tubercle; Mp, median plate; Pp, pedipalp; Pt, patella; T, tergites (numbered); Ti, tibia. Scale bar = 1 mm.

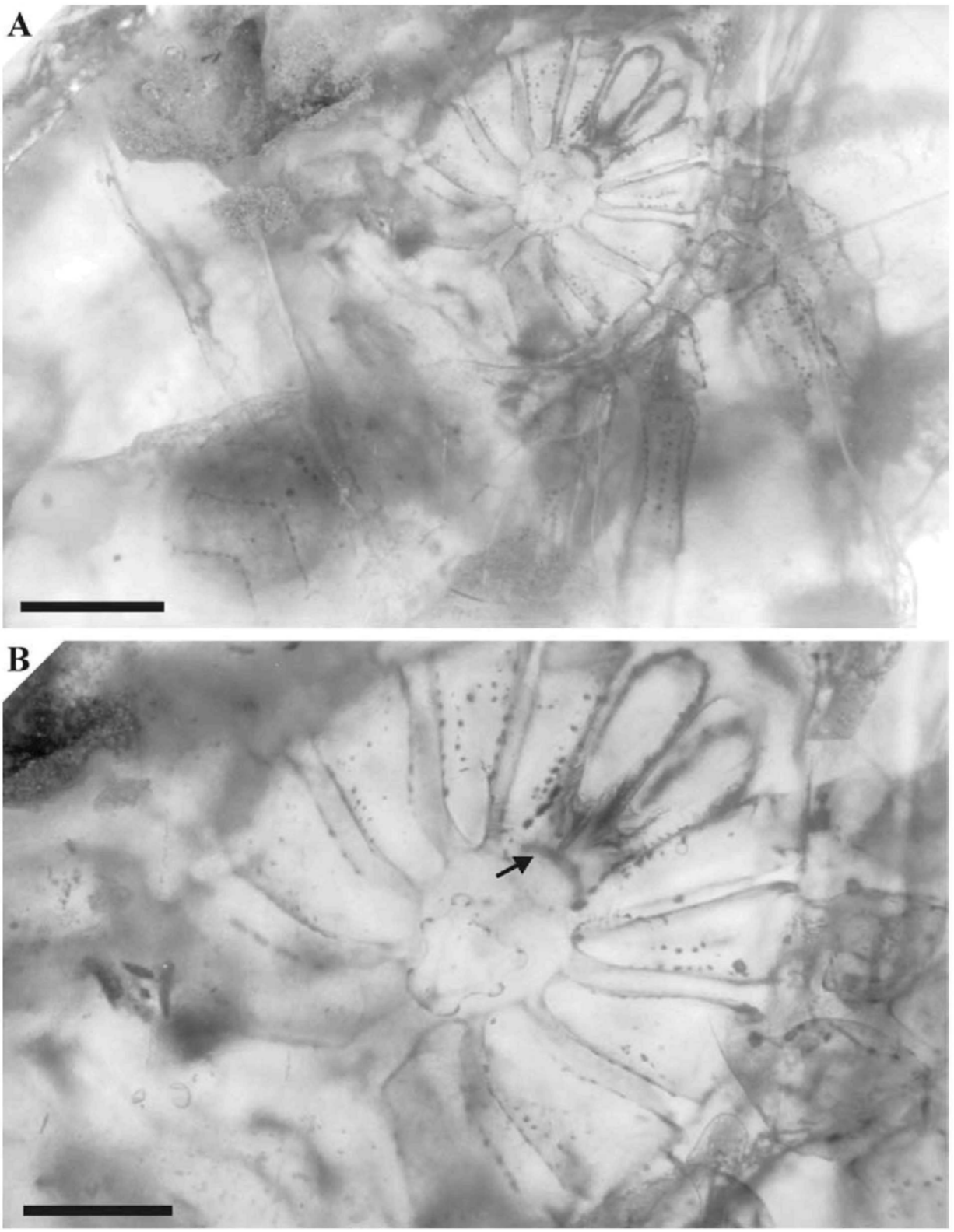

Figure 4 *Palaeocharinus tuberculatus* sp. nov., Pragian, Rhynie, Scotland. AUGD12409. **A**, Ventral view of the holotype. Scale bar = 1 mm. **B**, Close-up of ventral prosoma. The position of the labrum is arrowed. Scale bar = 0.50 mm.

most distinct and consistent of these polygons occur on the centre of the carapace, comprising a circle approximately 0.35 mm in diameter, posterior to a pair of more reniform shape, up to 0.35 mm in length (Fig. 3). Laterally, a row of well defined polygons occurs above each of the indentations of the lateral border (Figs 6A & 7A). These are defined by the rebordered lateral margin, a vertical row of microtubercles separating each indentation, and dorsally by a longitudinal row of microtubercles that pass anteriorly onto the lateral margins of the clypeus.

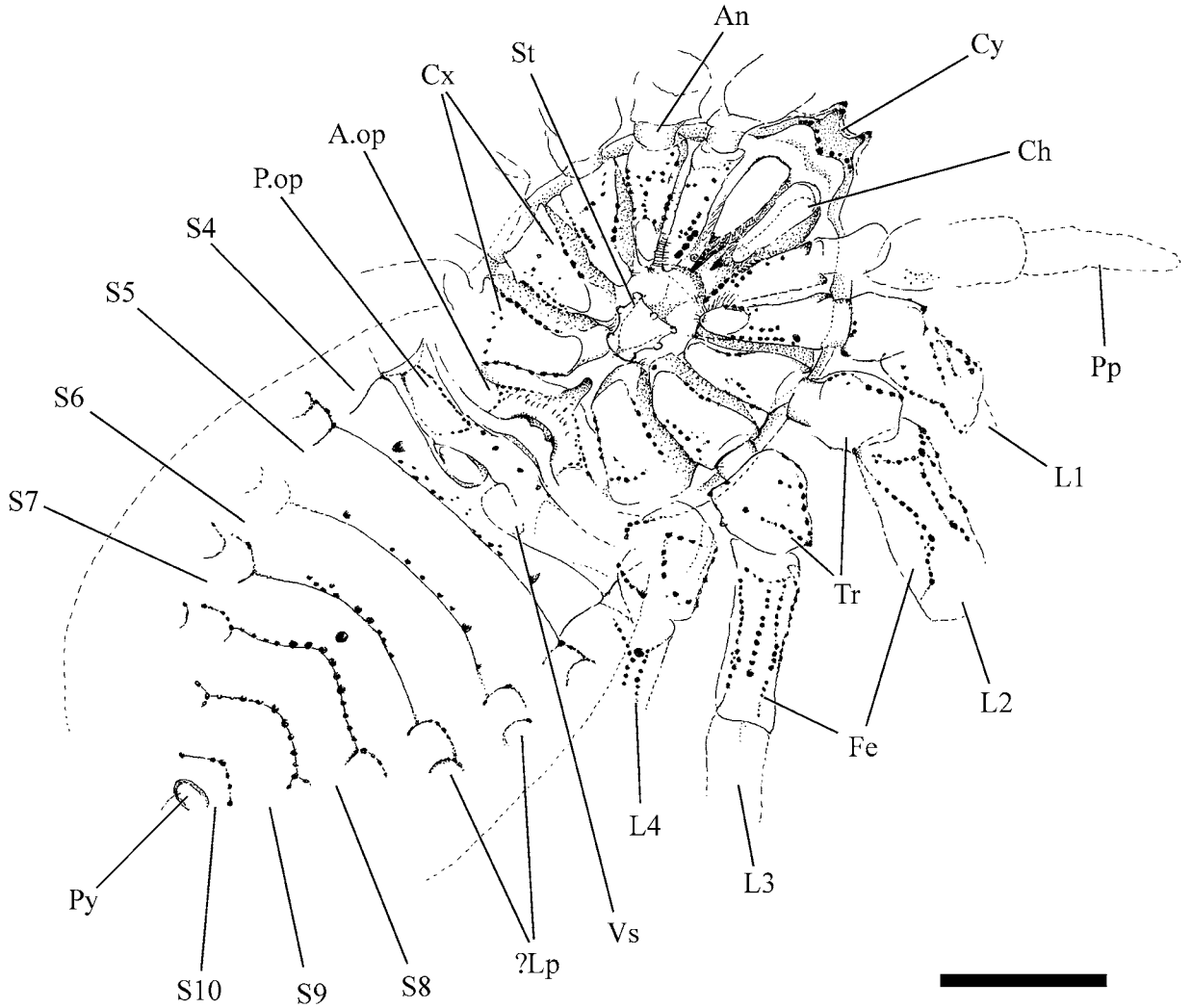

Figure 5 *Palaeocharinus tuberculatus* sp. nov., Pragian, Rhynie, Scotland. AUGD12409. *Camera lucida* drawing, *vide* Fig. 4A, showing the ventral anatomy. An, annulus; A.op, anterior operculum; Ch, chelicerae; Cy, clypeus; Fe, femur; L, walking legs (numbered); ?Lp, lateral plates; P.op, posterior operculum; Pp, pedipalp; Py, pygidium; S, sternites (numbered); St, sternum; Tr, trochanter; Vs, ventral sacs. Scale bar = 1 mm.

Ventral prosoma

The details of the ventral prosoma are clearest in the holotype (AUGD12409; Figs 4–5). The ventral prosoma comprises the coxae of the pedipalps and walking legs surrounding a well defined sternum. The posterior-most coxae (leg 4) are largest; the other leg coxae become progressively smaller anteriorly. The fourth coxae are approximately 0.83 mm in length, diverging posteriolaterally at an obtuse angle of approximately 130°. Proximally, they appear to have been partially separated in life by the median, anterior protrusion from the opisthosoma (see below). Posteriorly the fourth coxae fit snugly into corresponding depressions in the anterior operculum. The leg 3 coxae are approximately 0.77 mm in length, diverging laterally, perpendicular to the midline. The embayed shape of the anterior surface of the fourth coxae (Fig. 5) suggests that, in life, the third coxae were in contact with the fourth. The leg 2 coxae are approximately 0.74 mm in length and diverge anteriolaterally at about 140°. The leg 1 coxae diverge anteriolaterally at approximately 100° and are approximately 0.73 mm in length. The leg coxae are tuberculate, the second to fourth coxae each bearing a ridge of microtubercles on their anterior and posterior margins, with microtubercle size gradually increasing medially. An indistinct, staggered row of microtubercles also occurs on the ventral surface posterior to the distal margins of the coxae. The first coxae show the same ornament, but with a greater density of scattered microtubercles, proximally forming coarse granules on what is effectively a gnathobase. All coxae bear scattered sockets for macrosetae; the leg 1 coxae bearing dense tufts of plumose setae on the gnathobase (Fig. 5).

The pedipalpal coxae are approximately 0.80 mm in length, diverging anteriolaterally at 65°. They embrace the chelicerae and, like the leg coxae, have a pronounced, tuberculate ornament, mainly concentrated towards the anterior surface. A row of large granules occurs on the proximal, anterior margin of this gnathobasic coxal edge, the granules becoming larger in size proximally and mesially. The gnathobase on the palpal coxae also bears numerous plumose setae, as seen in other Rhynie trigonotarbids (Dunlop 1994*a*).

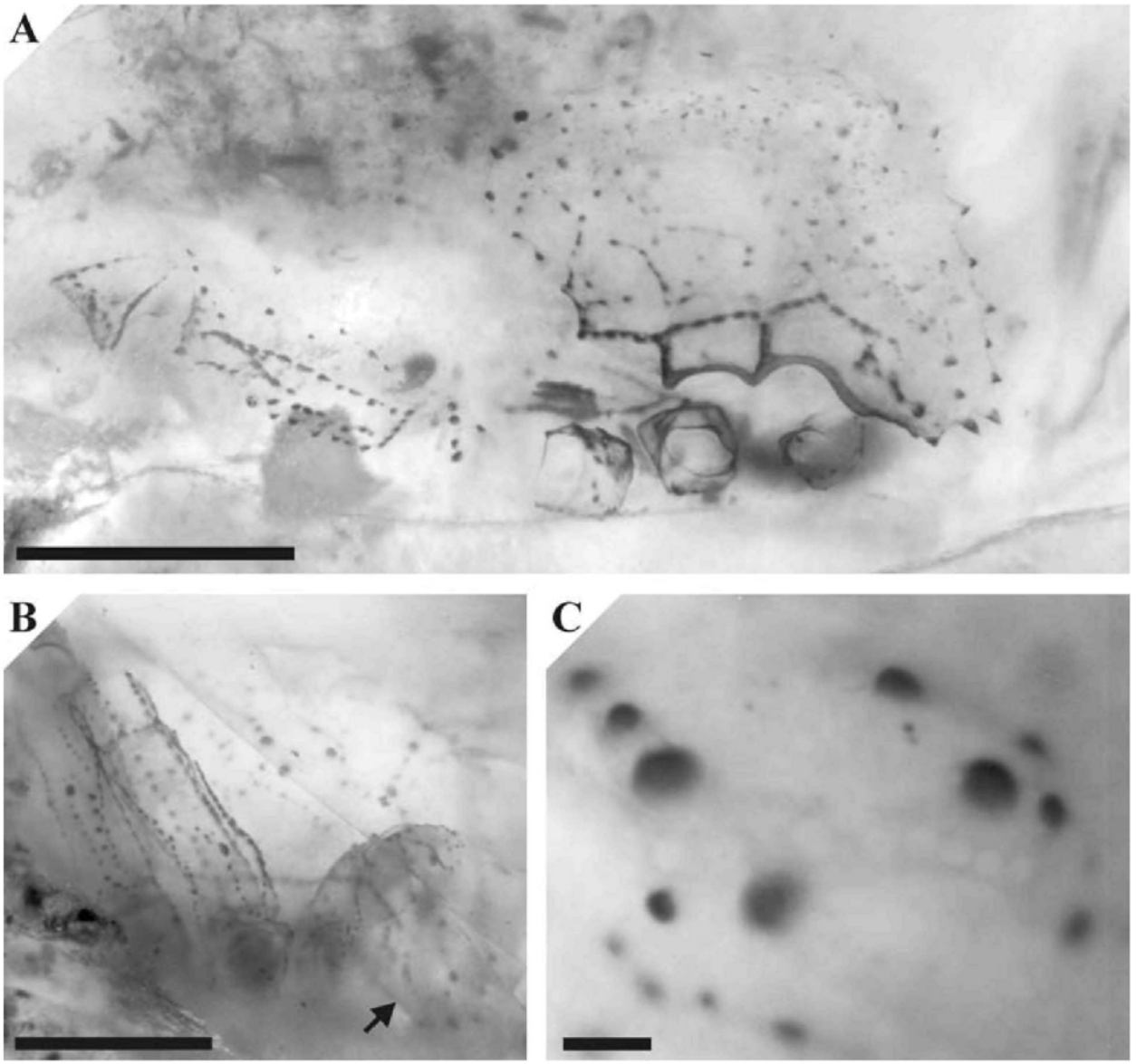

Figure 6 *Palaeocharinus tuberculatus* sp. nov., Pragian, Rhynie, Scotland. **A**, Anterior and left side of a prosoma, viewed from the internal aspect. AUGD12413. Scale bar = 1 mm. **B**, Anterior and right side of the prosoma of the holotype, showing the clypeus (arrowed) at depth within the chert. Notice the distinctive tuberculate ornamentation on the leg podomeres (left). AUGD12409. Scale bar = 1 mm. **C**, Close-up of the lateral eye tubercle in **B**, showing the distinctive tuberculate ornament and the position of the eye lenses. AUGD12409. Scale bar = 0.10 mm.

The sternum is broadly rectangular in outline, approximately 0.36 mm in length, and maximally 0.33 mm wide, but is strongly indented where the coxae attach. Indentations on the margins of the plate correspond with the first, second and third walking leg coxae. The posterior margin of the sternum lies in front of the fourth coxae and appears broadly rounded. The point between each coxal indentation is marked by a single, knob-like tubercle (Figs 4B & 5).

The exquisite preservation of the holotype and the transparency of the enclosing chert reveal further ventral details. Posterior to the chelicerae and anterior to the sternum, is a dark, arcuate piece of cuticle, quite deep within the specimen (Figs 4B & 5). Its shape and position would correspond with the upper mouth lip or labrum, a feature previously described from lateral sections of *Palaeocharinus* by Dunlop (1994*b*). Posterior to this feature and extending deep within the specimen, the anterior surface of the sternum can be resolved.

Opisthosoma

The three-dimensional preservation reveals the shape of the opisthosoma, as well as the disposition, morphology and ornament of the tergites and sternites. Again the holotype offers the best preservation (Figs 3, 4A, 5 & 8). The opisthosoma is broadly ovoid in shape, at its widest point around the sixth tergite up to 2.70 mm wide, thus being almost one-third longer than wide. Ventrally it is strongly convex (Fig. 8), the sternites being generally wider than the corresponding tergites. The dorsal surface in the holotype also appears rather convex giving the opisthosoma a distended appearance. This differs from other complete palaeocharinids found in the chert where

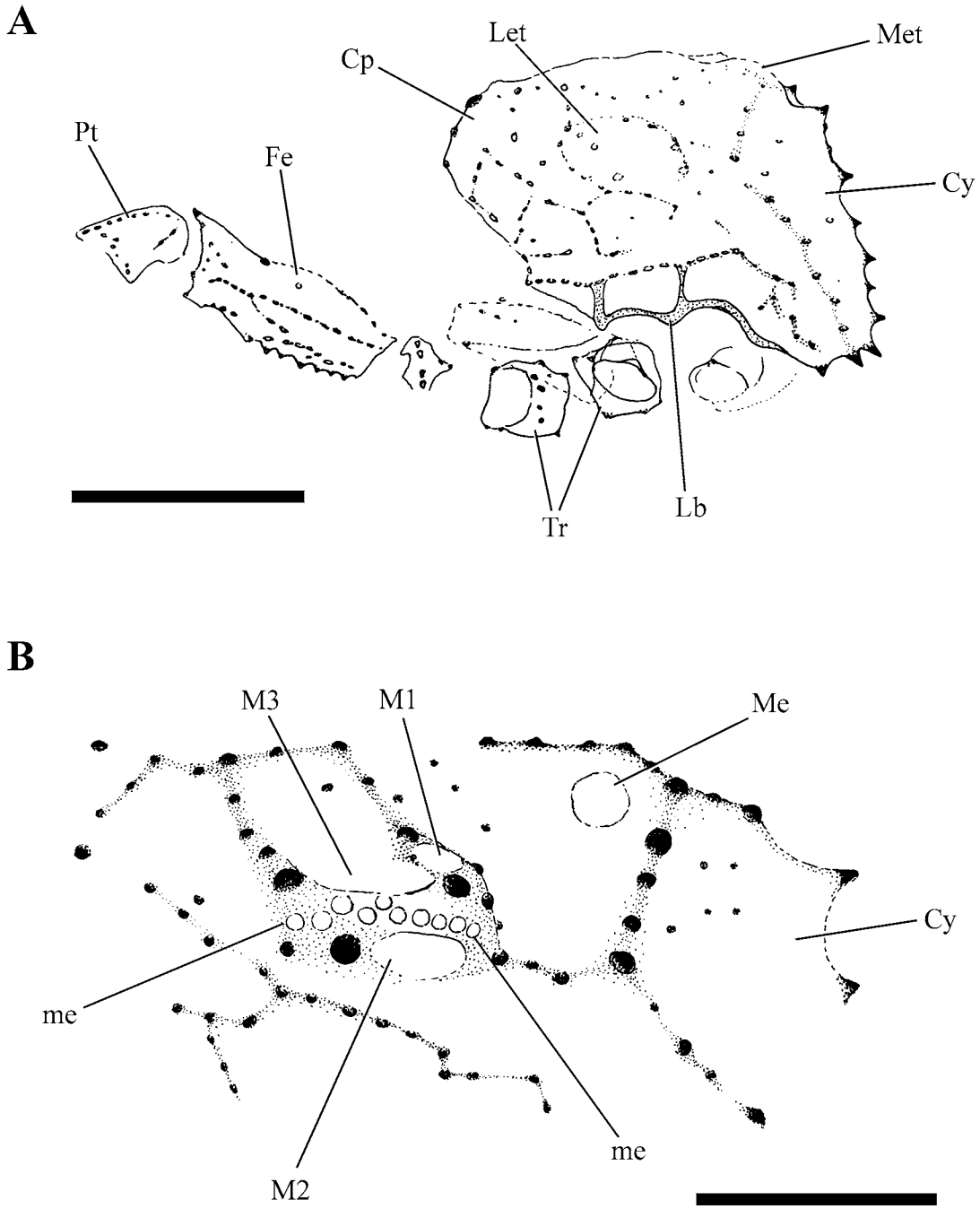

Figure 7 *Palaeocharinus tuberculatus* sp. nov., Pragian, Rhynie, Scotland. **A**, *Camera lucida* drawing, *vide* Fig. 6A, showing the rebordered lateral margin of the carapace (Lb) and the disposition of the lateral eye (Let) and median eye (Met) tubercles. For other abbreviations please see the legends to Figs 3 & 5. AUGD12413. Scale bar = 1 mm. **B**, *Camera lucida* drawing, *vide* Figs 6B & 6C, illustrating the disposition of the eye lenses on the median and lateral eye tubercles. Cy, clypeus; Me, median eye (right lens); M1, posterior median lens; M2, anterior lateral lens; M3, posterior lateral lens; me, minor eye lenses (10 in all, separating lens M2 from lenses M1 and M3). AUGD12409. Scale bar = 0.50 mm.

the dorsum of the opisthosoma typically appears flattened to slightly concave.

The dorsum comprises nine tergites. With the exception of the ninth and, possibly, the first tergite, each is divided into a broad median sclerite with two smaller lateral ones (Figs 3 & 8). Of these tergites, the median plates are more or less the same width from tergites T2 + 3 to T6, but decrease in width from T7 to T8 (Fig. 3). The tergites appear to be slightly separated in the holotype (AUGD12409): (Fig. 3) and paratype AUGD12412, perhaps as a result of postmortem decay. In an undistended animal in life the anterior tergites probably slightly overlapped the posterior ones, with the median plates slightly overlapping the corresponding lateral plates.

As in other *Palaeocharinus* material, the first tergite is longest along the midline, *c.* 0.48 mm. The anterior portion lies in a corresponding fold beneath the posterior margin of the carapace, where it forms an interlocking ridge (Fig. 3; see Shear *et al.* 1987: fig. 4). An ornament of circular pits

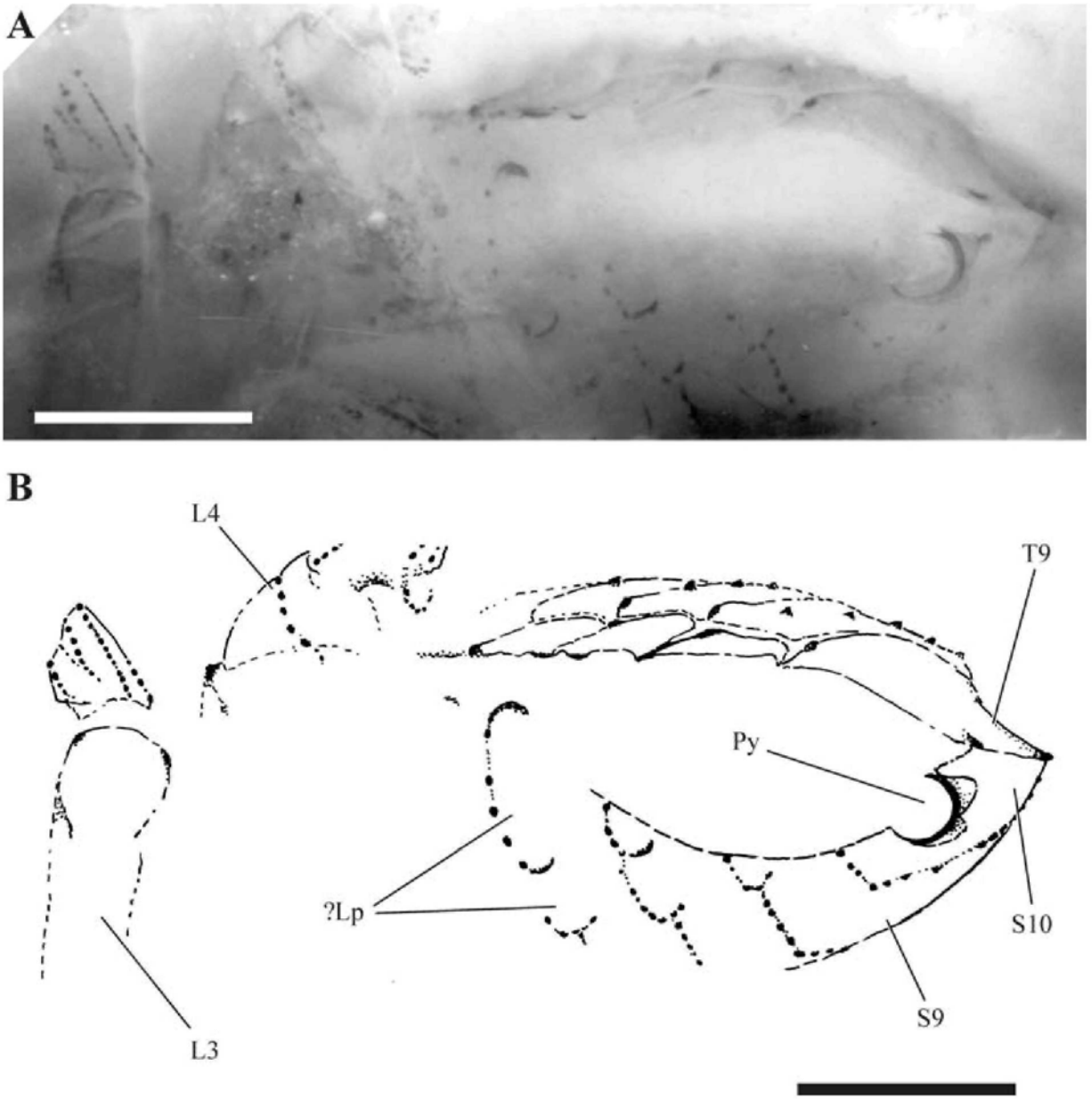

Figure 8 *Palaeocharinus tuberculatus* sp. nov., Pragian, Rhynie, Scotland. AUGD12409. **A**, Posteriolateral view of the opisthosoma and remains of the third and fourth walking legs (left side) of the holotype. Notice the convex nature of the tergites giving the opisthosoma a distended appearance. Scale bar = 1 mm. **B**, *Camera lucida* drawing showing the possible relic lateral plates of the sternites (?Lp). For other abbreviations please see the legends to Figs 3 & 5. Scale bar = 1 mm.

occurs on tergite 1, where it is exposed behind the carapace, comprising a large, central depression flanked on either side by two, possibly three further smaller depressions. Posterior to this, a narrow band of cuticle either representing the posterior border of the first tergite, or anterior border of the second, has a single row of evenly spaced microtubercles, each apparently protecting a small, socketed seta. Laterally, this narrow band expands into small triangular areas, apparently flanking the first tergite and curving posteriolaterally to partially flank the anterior part of the second tergite. These triangular areas may represent small lateral plates belonging to the first tergite.

The second and third tergites are fused together into a macrotergite (see Shear *et al.* 1987 for a discussion and justification) and together form the longest plate on the dorsum, *c.* 0.52 mm. The width of this tergite is 2.24 mm. The approximate lengths and maximum widths, respectively, for the fourth to eighth tergites are as follows: T4 = 0.40 mm and 2.58 mm, T5 = 0.40 mm and 2.65 mm, T6 = 0.40 mm and 2.70 mm, T7 = 0.38 mm and 2.64 mm and T8 = 0.32 mm and 2.20 mm. The ninth tergite (T9) is entire and undivided (Figs 3B & 8), its length is approximately 0.45 mm and at its maximum width it is 1.55 mm, where it joins the previous tergite (T8).

The ornament of the tergites is quite distinctive, appearing tuberculate, quite unlike existing *Palaeocharinus* specimens (Hirst 1923). In common with other Rhynie trigonotarbids there are paired circular depressions (?muscle

apodemes) in the middle of tergites T2 + 3 and the paired depressions on the anterior borders of tergites T4–8 (Fig. 3; see Shear *et al.* 1987: fig. 4). A smaller, central depression also occurs on the anterior border of tergites T4–8 on the midline of the opisthosoma (Fig. 3B). The tuberculation is near symmetrical. The anterior border of each median plate is fringed by almost evenly placed microtubercles, either side of and between the depressions described above. Towards the posterior of each median plate is a staggered row of typically eight microtubercles, decreasing to four on tergite T8. The lateral edges of the median plate of tergites T2 + 3 also support a single row of microtubercles. Smaller microtubercles appear scattered over the rest of the surface of the median plates, but locally appear to form a central, single staggered row across the width of the median plates in tergites T5 and T6 (Fig. 3B).

The lateral and posterior margins of the lateral plates are fringed by up to four microtubercles, with minor smaller microtubercles scattered across the surface. Of interest, however, is the consistent presence of two larger, tear drop-shaped microtubercles on each lateral plate (T2 + 3 to T8) positioned in a line, approximately a third of the plate width, in from the lateral margin (Fig. 3). This gives the lateral plates the appearance that they are longitudinally subdivided. A dark, tear drop-shaped area also occurs in the anterior, medial corner of each lateral plate (Fig. 3). All the larger microtubercles appear to flank, or are positioned anterior to, a socketed seta. The posterior margin of the ninth tergite (T9) bears two spine-like microtubercles, similar to that seen in the other *Palaeocharinus* species, as well as a row of five microtubercles positioned just anterior to the posterior border (Fig. 8).

Ventral opisthosomal morphology (Figs 4A, 5 & 8) is similar to that of previous *Palaeocharinus* specimens, but there are some significant differences. Widths of sternites given here are as viewed from below and do not account for their strong curvature. The first sternite may be absent, a possible trigonotarbid autapomorphy (Dunlop 1994*b*), but could be hidden above and behind the fourth coxae at depth within the matrix. Following Shultz's (1993) comparative study of Uropygi, the second and third 'sternites' of trigonotarbids associated with the book lungs are tentatively equated to highly modified, flattened, lung-bearing appendages: the anterior and posterior opercula (Dunlop 1996*b*, *c*). The anterior operculum is approximately 0.40 mm in length, along the median line, and approximately 1.90 mm in width. The anterior margins are embayed to accommodate the leg 4 coxae; an acute median, anterior protrusion of the plate extends between the proximal, posterior medial surfaces of the fourth coxae (Fig. 5). The posterior margin of the anterior operculum is indented medially, showing a darkened strip of apparently folded cuticle (Figs 4 & 5). Medially, the anterior operculum is covered with short setae and the anterior of the plate is marked by a row of microtubercles (Fig. 5).

The posterior operculum is approximately 0.43 mm in length along the midline and approximately 2.26 mm in width and it bears a pair of ovate ventral sacs (Fig. 5). Anterior to the ventral sacs is a transverse row of four microtubercles; anteriolaterally, extending towards the lateral margins of the median plate, a rectangular pattern is formed on either side by a single row of microtubercles (Fig. 5). The fourth sternite (S4) appears narrower along the midline (approximately 0.17 mm), where it is embayed to accommodate the ventral sacs of the posterior operculum. The posterior margin of this sternite is also broadly convex towards the anterior. Both the posterior operculum and sternite S4 appear to be laterally divided into a broad median plate flanked each side by a short lateral plate (Fig. 5). The total width of sternite S4, as viewed, is approximately 2.57 mm. A pair of large microtubercles occurs on sternite S4, posteriolaterally to the ventral sacs. Medial to these is a staggered row of smaller microtubercles on the posterior margin of the sternite. These and all the tuberculation described below for the posterior sternites, show a near symmetry about the midline of the opisthosoma.

From sternites S5 to S9, the plates become progressively more chevron-like in their appearance towards the posterior of the opisthosoma, where what is interpreted to be the tenth sternite (S10), bearing the pygidium, appears to form a triangular plate flanked by the curvature of the ninth sternite (S9) (Figs 5 & 8). The lateral edges of sternite S9 and the posterior edge of the triangular sternite S10 meet the edges of tergite T9. The approximate midline lengths of sternites S5–9 are as follows: 0.43 mm, 0.42 mm, 0.32 mm, 0.45 mm and 0.45 mm respectively (Fig. 5), although the lengths of sternites S7 to S9 are probably slightly longer considering the curvature of the ventral opisthosoma. When viewed from the left, posteriolateral aspect (Fig. 8), the length of the triangular sternite S10 is 0.80 mm along the midline. The posterior borders of sternites S5 to S9 are fringed by a single row of microtubercles, apparently most numerous on sternite S7 (Fig. 5). This sternite also has a single, larger tubercle positioned on the midline of the plate. Interestingly, the lines of tuberculation on the posterior borders of these sternites, with the exception of sternite S9, appear to bifurcate twice when traced towards the lateral margin of the opisthosoma (Figs 5 & 8), the posteriorly directed line of microtubercles in both 'bifurcations' terminating within the successive posterior sternite. Although there is no evidence of distinct sutures, the two-fold bifurcation in the lines of microtubercles gives the impression of a pseudodivision into lateral plates.

The pygidium is positioned in the centre of sternite S10 and is approximately 0.34 mm in diameter (Figs 5 & 8). The edge of the ring appears to be slightly rebordered (Fig. 8A). The fragmentary remains of what appear to be two plates are attached ventrally and dorsally to the edges of the ring and probably equate to segments 11 and 12 (Fig. 8).

Appendages

Podomeres associated with the specimens have a characteristic ornament, quite distinct from those of other *Palaeocharinus* species. The chelicerae have only been seen on the holotype (Figs 4 & 5). In this specimen the fangs have been truncated by the thin section, although the tip of the right fang remains, suggesting they were long, curved and sabre-like. Cheliceral teeth are present, comprising one large tooth and at least two smaller ones. The mesal surfaces of the chelicerae are covered by dense, plumose setae.

The pedipalps are most complete in the holotype (Figs 4A, 5 & 6B), although given their depth within the chert details remain equivocal. The distal portion of a possible pedipalp, slightly truncated by the thin section, is present together with other articulated leg appendages in paratype AUGD12411. Excluding the coxae, the

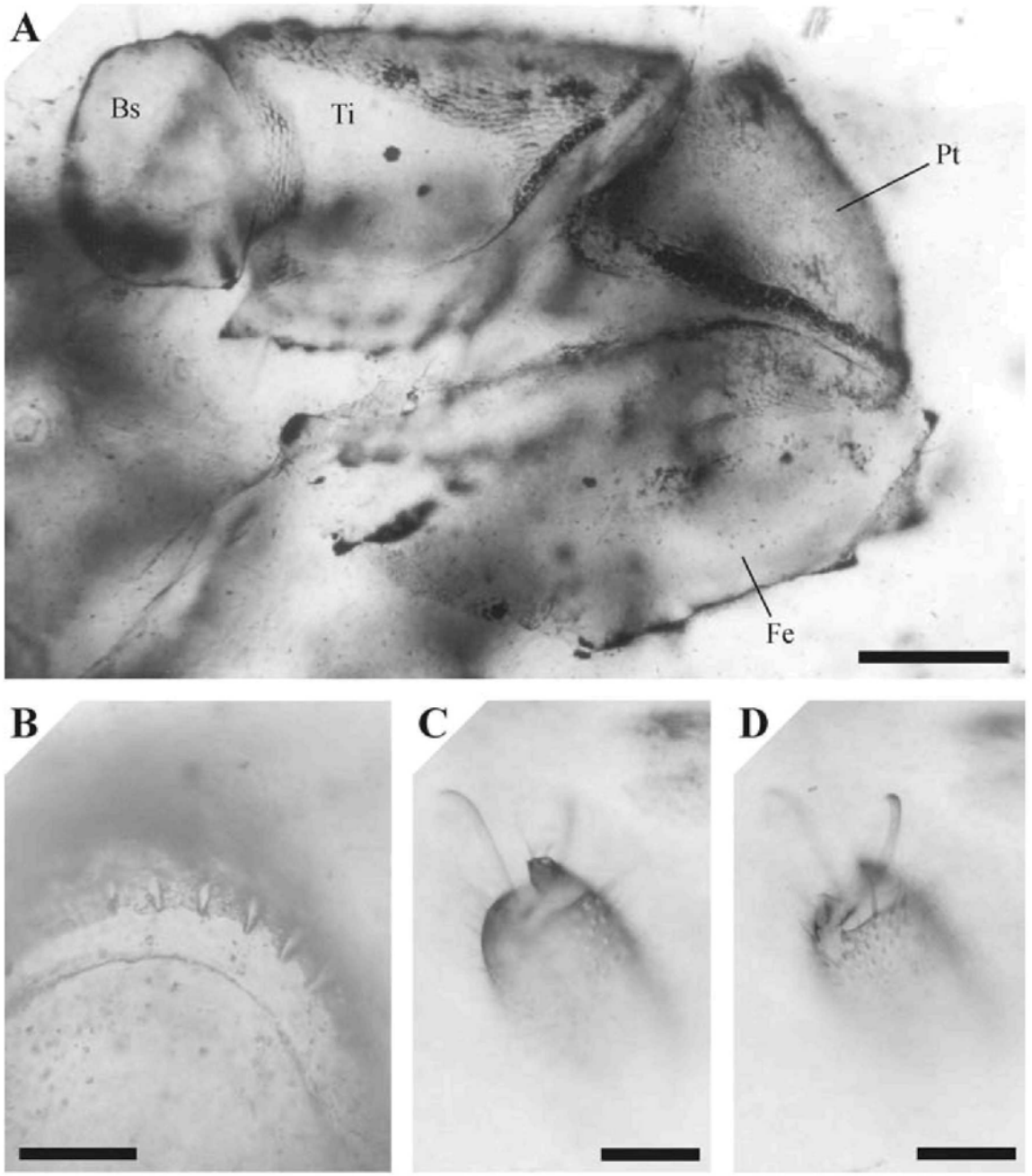

Figure 9 *Palaeocharinus tuberculatus* sp. nov., Pragian, Rhynie, Scotland. **A**, Partial femur (Fe), patella (Pt), tibia (Ti) and basitarsus (Bs) of a walking leg. AUGD12411. Scale bar = 0.20 mm. **B**, Close-up of slit sense organs on the distal extremity of a basitarsus. AUGD12411. Scale bar = 0.05 mm. **C**, Distal extremity of a telotarsus and claws. **D**, Same view as **C**, at a deeper level of focus, showing dense setae on the surface of the telotarsus. AUGD12410. Scale bar = 0.20 mm.

pedipalps are approximately 2.23 mm in length and each comprises five additional articulated podomeres: a trochanter, femur, patella, tibia and an undivided tarsus. The width of the pedipalps gently tapers towards the distal end of the tarsus. The approximate lengths of the respective, individual podomeres are as follows: 0.43 mm (trochanter), 0.43 mm (femur), 0.43 mm (patella), 0.38 mm (tibia) and 0.56 mm (tarsus). It is not clear from the specimens whether the tarsus bears a single apical claw as observed in other *Palaeocharinus* material. The pedipalps, like the legs, display a conspicuous, microtuberculate ornament (see below), although the inferior surfaces of the tibia and tarsus observed in the paratype AUGD12411 appear to lack such an ornament.

In none of the specimens are the legs complete, or entirely visible, due to postmortem fragmentation, thin section preparation and the depth of the elements within the chert. The specimen showing the most complete leg appendages is again the holotype (Figs 3, 4A, 5 & 6B). Other specimens are more fragmentary, but show further details of individual podomeres, their ornamentation, setation and articulation (Fig. 9). Each leg, excluding the coxae, comprises 6

podomeres: a trochanter, femur, patella, tibia, basi- (or meta-) tarsus and telotarsus.

With the possible exception of the palpal tibiae and tarsi, the palpi and legs exhibit a conspicuous ornament that, again, distinguishes them from those of *Palaeocharinus*. Generally the ornament comprises pronounced parallel to subparallel, longitudinal rows of robust, distally directed, thorn-like microtubercles (Fig. 9A). A single row of similar microtubercles fringes the distal and proximal margins of all the podomeres, with the exception of the telotarsi on which one poorly defined row of microtubercles occurs on the proximal margin of the podomere. The tuberculation is further described for each podomere (see below).

The trochanters (Figs 4, 5, 6A & 7A) are relatively large. The approximate, respective lengths for those of the first to the fourth (posterior most) legs being: 0.50 mm, 0.54 mm, 0.60 mm and 0.66 mm. The superior surface of the trochanters are approximately two-thirds the length of the inferior surface, so that the distal joint plane is superiorly directed. Few setae are present scattered over the surface. The disposition of the longitudinal rows of microtubercles is not entirely clear due to the orientation of the podomeres and the depth of the specimens within the chert matrix, but there appears to be at least one row on the anterio-inferior and posterio-inferior surfaces and possibly a further row on the superior surface.

A circular annulus, 0.10–0.12 mm long, separates the trochanter from the coxa on each leg and what appears to be a shorter annulus separates the trochanter from the femur (Figs 4A & 5). The articulations of the coxa–trochanter and trochanter–femur joints and associated annuli are not particularly clear in any of the specimens. However, from the slightly darkened areas of cuticle seen on these podomere joints in the holotype, it would appear the articulations are superio-posterior and anterio-inferior at both joints.

The femora of the walking legs (Figs 4A, 5, 6A, 6B, 7A & 9A) comprise the longest podomeres, increasing in length from the first to the fourth walking legs, the approximate lengths in the holotype being: 1.14 mm, 1.17 mm, 1.25 mm and 1.34 mm, respectively. Setae are few and increase in number distally. The distal joint plane is inferiorly directed, bearing a superior bicondylar hinge.

The ornament of the femora comprises three longitudinal, subparallel rows of microtubercles on the superior surface, each terminating in a projecting spine on the distal margin of the podomere. Two longitudinal rows of microtubercles occur on the inferior surface, diverging from an inflection in the single row of microtubercles that fringes the proximal margin. Of these, the posterior row generally terminates approximately two-thirds along the length of the podomere. On both the anterior and posterior surfaces is another microtubercle row, each beginning at the proximal margin, curving downwards onto the inferior surface and back to terminate towards the distal margin.

The patellae (Figs 3B, 6A, 7A & 9A) are not complete for all walking legs, but appear to range between 0.46–0.56 mm in length, with the inferior surface being considerably shorter than the superior surface, resulting in both proximal and distal joint planes being inferiorly directed. The distal articulation is a superior bicondylar hinge.

The ornamentation comprises three longitudinal, parallel rows of microtubercles on the superior surface, each terminating with a projecting spine on the distal margin. Few setae are present and are mainly scattered over the superior surface.

The tibiae (Figs 3 & 9A) range between 0.56 mm (AUGD12411: Fig. 9A) and 0.84 mm (AUGD12409: Fig. 3) in length. The inferior surface is approximately two-thirds the length of the superior surface, the proximal joint plane appearing inferiorly directed. The distal articulation appears to be a superior bicondylar hinge.

The superior surface of the tibiae bears four longitudinal, subparallel rows of microtubercles. The inferior surface bears two longitudinal, subparallel rows of microtubercles. The latter each terminate in a large spine on the distal margin of the podomere (Fig. 9A), comparable with those seen on the corresponding podomeres seen in other palaeocharinids from the chert. Setae are rather more common, being scattered over the surface of the podomere.

The basitarsi (Figs 3, 9A & 9B) are cylindrical and relatively short (approximately 0.23 mm in length). The distal joint appears to be a superior hinge, although further details of the articulation are unclear. The superior surface bears three longitudinal, subparallel rows of microtubercles. Tuberculation on the inferior surface is not clear in the specimens. These podomeres bear numerous setae. The distal margins of the basitarsi bear a single row of slit sensillae (Fig. 9B).

The telotarsi of the walking legs (Figs 9C & 9D), observed in specimens AUGD12410, AUGD12411 and AUGD12412, appear to be two to three times longer than wide and terminate with an articulated pair of sickle-like apical claws or ungules. Superior to and between the claws is a small, median protrusion, bearing a pair of tiny setal sockets (Fig. 9C). Two or three short longitudinal, subparallel rows of microtubercles on the superior surface are confined to the proximal portion of the podomeres. The telotarsi are covered by a dense array of socketed setae.

DISCUSSION

A reconstruction of *Palaeocharinus tuberculatus* is presented in Fig. 10, together with a comparative reconstruction of one of Hirst's more complete species, *Palaeocharinus rhyniensis*. The reconstruction of the new trigonotarbid is based primarily on the specimens described above, but draws on other palaeocharinid material.

At *c.* 6–7 mm in body length, our new specimens are almost twice the size of Hirst's original palaeocharinids from Rhynie. Still larger trigonotarbids, with body lengths of up to 14 mm, are known from the cherts (e.g. Rolfe 1985: fig. 6; Dunlop 1994*b*: pl. 42). They are preserved in very thin sections in which gross morphological characters are hard to see and have never been formally described and diagnosed. These largest specimens may represent a new genus (pers. obs.) and will be treated in a separate publication. The distinctive tuberculate ornament in *Palaeocharinus tuberculatus* is unlike anything seen in Hirst's original material and is a convincing autapomorphy of our new species. We feel it is unlikely that our new fossils are more advanced instars and/or sexually dimorphic examples of previous Rhynie species, since among living arachnids such a marked difference in body ornament rarely occurs between the sexes, or between growth stages. It is still not possible to assign Rhynie fossils to males or females.

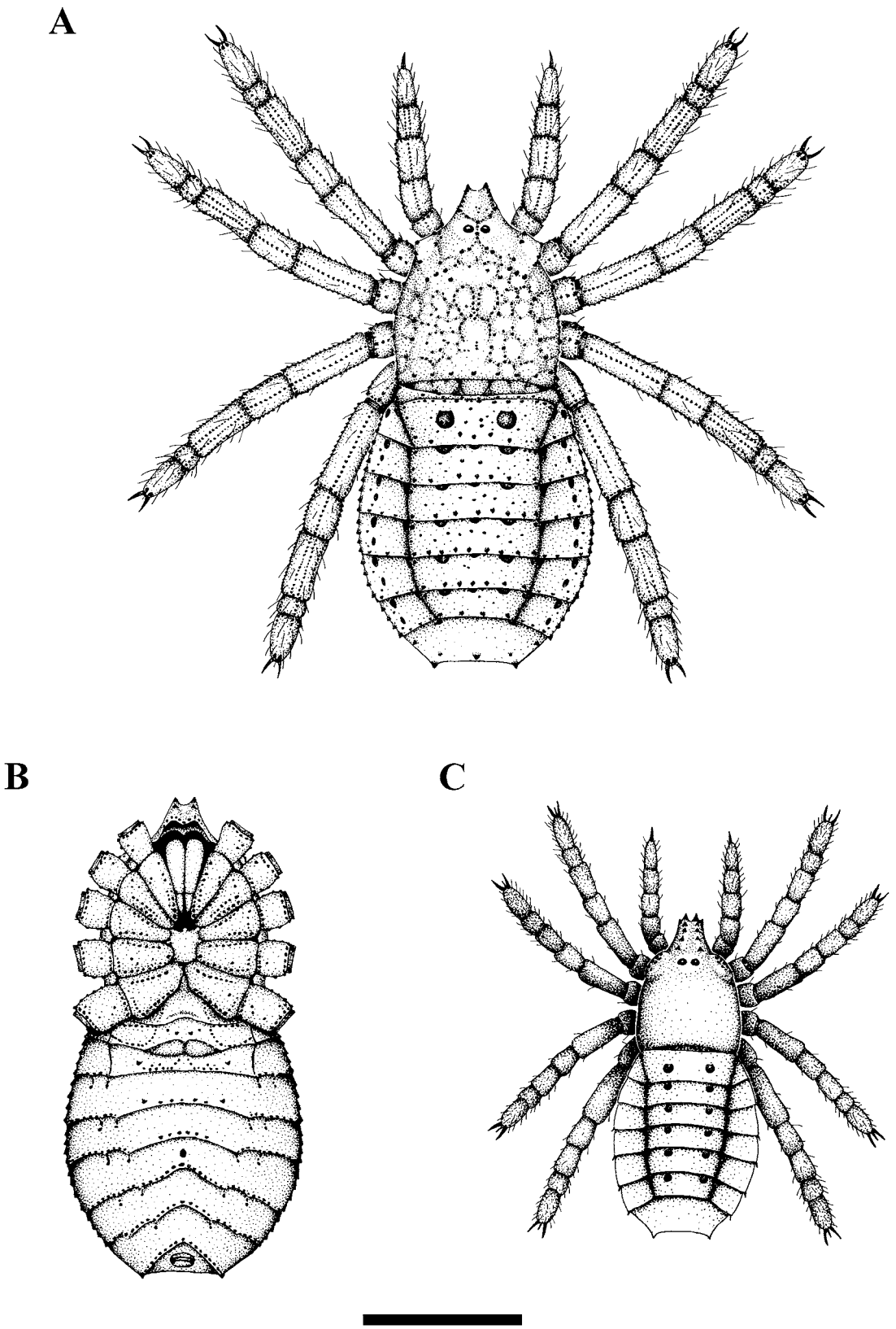

Figure 10 Reconstructions of palaeocharinids from the Windyfield chert. **A**, *Palaeocharinus tuberculatus*, sp. nov., dorsal view. **B**, *Palaeocharinus tuberculatus*, sp. nov., ventral view. Walking legs and pedipalps omitted. **C**, *Palaeocharinus rhyniensis* Hirst, 1923, dorsal view, drawn to scale with **A** and **B**. Modified from Dunlop (1996*b*). Scale bar = 2 mm.

With regard to the opisthosoma morphology, as with other *Palaeocharinus* species this animal shows what appears to be a tenth sternite (S10), fused with the chevron-like ninth sternite (S9), the remaining demarcation highlighted by the row of microtubercles along the posterior margin of S9. The corresponding tenth tergite is either lacking or has fused with either the ninth tergite (T9) or, perhaps most likely given the ring-like nature of segment 10 in other tetrapulmonates (e.g. Shultz 1993), with the tenth sternite to effectively form a single (10th) sclerite surrounding the pygidium. The presence of two further segments (11–12) within the pygidial socket would produce a 12-segmented opisthosoma, in agreement with the reconstruction in Dunlop (1996*a*). The convexity of the opisthosoma in this new material (Fig. 8A) is intriguing. It is not seen in Hirst's fossils and it remains unclear whether the morphology observed here reflects the condition of the opisthosoma in life. In living arachnids the opisthosoma can become quite bloated and distended after a large meal or in a gravid female and the sclerites become separated from one another to reveal the soft membranes between them (pers. obs). Alternatively, we could be looking at some sort of postmortem swelling of the body prior to silicification.

The acute anterior projection on the anterior operculum of *P. tuberculatus* is also seen in the other palaeocharinids from the cherts at Rhynie. Its function is unclear, but together with the posterior of the fourth coxae and their corresponding embayments on the anterior operculum it appears to form part of the ventral locking mechanism between the prosoma and opisthosoma. A similar anterior projection is seen in the Ricinulei (Dunlop 1996*c*), also forming part of the ventral locking mechanism, but there it is rounded and far less pronounced. The darkened strip of folded cuticle on the medially indented posterior margin of the anterior operculum may represent the position of the gonopore opening. In all other arachnids, with the possible exception of the Ricinulei, the gonopore opens on the second opisthosomal somite (Dunlop 1996*c*), as could conceivably be the case here.

The longitudinal subdivision of the opisthosomal tergites and sternites is of particular interest. Dunlop (1994*b*, 1996*b*) speculated that the Rhynie palaeocharinids could be closely related to the Carboniferous family Anthracomartidae (but see Shear 2000 for criticisms). Although previously considered to be a separate and unrelated order (*sensu* Petrunkevitch 1949), anthracomartids are *bone fide* trigonotarbids, specifically with a similar carapace shape to Rhynie palaeocharinids. Characteristically, anthracomartids have a micro-ornament of fine tubercles over the entire body, they have tergites composed of 5 plates – not 3 as in other trigonotarbids – and they have divided sternites with the divisions effectively forming a broad marginal rim around the ventral opisthosoma. In our new palaeocharinid fossils there is a general pattern of dispersed microtubercles and the specific tuberculation on the lateral plates hints at a further lateral subdivision of these sclerites, equivalent to the anthracomartid condition. However, no demarcation line or break in the cuticle is present in the Rhynie fossils. It is tempting to see these pseudodivisions of the lateral plates in *P. tuberculatus* as foreshadowing a complete division in the Anthracomartidae. Furthermore, in *P. tuberculatus* not only are the posterior operculum and S4 subdivided laterally (as seen in other species of *Palaeocharinus*), but sternites S5–9 exhibit a tuberculation pattern that is suggestive of an anthracomartid-like pseudodivision of all the ventral plates. Again the Devonian *P. tuberculatus* approaches the Carboniferous anthracomartid condition, but in the absence of a phylogenetic framework for the entire Trigonotarbida we cannot take this hypothesis here further.

ACKNOWLEDGMENTS

S.R.F. was funded by the Lyon Bequest to the University of Aberdeen. Walter Ritchie and Barry Fulton are thanked for technical assistance. Lyall Anderson is thanked for useful discussions. The manuscript benefitted from helpful comments given by two anonymous referees.

REFERENCES

Anderson. L. I. & Trewin, N. H. 2003. An Early Devonian arthropod fauna from the Windyfield chert, Aberdeenshire, Scotland. *Palaeontology* **46**: 467–509.

Brock, T. D. 1994. *Life at high temperatures*. Yellowstone Association for Natural Science, History and Education, Inc., Yellowstone National Park, Wyoming, 31 pp.

Claridge, M. F. & Lyon, A. G. 1961. Lung-books in the Devonian Palaeocharinidae (Arachnida). *Nature* **191**: 1190–1191.

Cleal, C. J. & Thomas, B. A. 1995. *Palaeozoic palaeobotany of Great Britain*. Chapman and Hall, London, 295 pp.

Dunlop, J. A. 1994*a*. Filtration mechanism in the mouthparts of tetrapulmonate arachnids (Trigonotarbida, Araneae, Ampblypygi, Uropygi, Schizomida). *Bulletin of the British Arachnological Society* **9**: 267–273.

— 1994*b*. *Palaeobiology of the trigonotarbid arachnids*. PhD thesis, University of Manchester, UK.

— 1996*a*. A trigonotarbid arachnid from the Upper Silurian of Shropshire. *Palaeontology* **39**: 605–614.

— 1996*b*. Systematics of the fossil arachnids. *Revue Suisse de Zoologie* **103**: 173–184.

— 1996*c*. Evidence for a sister group relationship between Ricinulei and Trigonotarbida. *Bulletin of the British Arachnological Society* **10**: 193–204.

Fayers, S. R. 2003. *The biota and palaeoenvironments of the Windyfield chert, Early Devonian, Rhynie, Scotland*. PhD thesis, University of Aberdeen, UK.

Hirst, S. 1923. On some arachnid remains from the Old Red Sandstone (Rhynie chert Bed, Aberdeenshire). *Annals and Magazine of Natural History (Series 9)* **12**: 455–474.

Petrunkevitch, A. I. 1949. A study of Palaeozoic Arachnida. *Transactions of the Connecticut Academy of Arts and Sciences* **37**: 69–315.

Rice, C. M., Ashcroft, W. A., Batten, D. J., Boyce, A. J., Caulfield, J. B. D., Fallick, A. E., Hole, M. J., Jones, E., Pearson, M. J., Rogers, G., Saxton, J. M., Stuart, F. M., Trewin, N. H. & Turner, G. 1995. A Devonian auriferous hot spring system, Rhynie, Scotland. *Journal of the Geological Society, London* **152**: 229–250.

—, Trewin, N. H. & Anderson, L. I. 2002. Geological setting of the Early Devonian Rhynie cherts, Aberdeenshire, Scotland: an early terrestrial hot spring system. *Journal of the Geological Society, London* **159**: 203–214.

Rolfe, W. D. I. 1980. Early invertebrate terrestrial faunas. Pp. 117–157 *in* A. L. Panchen (ed.) *The terrestrial environment and the origin of land vertebrates*. Academic Press, London and New York.

— 1985. Early terrestrial arthropods: a fragmentary record. *Philosophical Transactions of the Royal Society of London (Series B)* **309**: 207–218.

Rößler, R., Dunlop, J. A. & Schneider, J. 2003. A redescription of some poorly known Rotliegend arachnids from the Lower Permian (Asselian) of the Ilfeld and Saale Basins, Germany. *Paläontologische Zeitschrift* **77**: 417–427.

Shear, W. A. 2000. *Gigantocharinus szatmaryi*, a new trigonotarbid arachnid from the Late Devonian of North America (Chelicerata, Arachnida, Trigonotarbida). *Journal of Palaeontology* **74**: 25–31.

—, **Selden, P. A., Rolfe, W. D. I., Bonamo, P. M. & Grierson, J. D.** 1987. New terrestrial arachnids from the Devonian of Gilboa, New York (Arachnida, Trigonotarbida). *American Museum Novitates* **2901**: 1–74.

Shultz, J. W. 1990. Evolutionary morphology and phylogeny of Arachnida. *Cladistics* **6**: 1–38.

— 1993. Muscular anatomy of the giant whipscorpion *Mastigoproctus giganteus* (Lucas) (Arachnida: Uropygi) and its evolutionary significance. *Zoological Journal of the Linnean Society* **108**: 335–365.

Trewin, N. H. 1994. Depositional environment and preservation of biota in the Lower Devonian hot-springs of Rhynie, Aberdeenshire, Scotland. *Transactions of the Royal Society of Edinburgh: Earth Sciences* **84**: 433–442.

— 1996. The Rhynie cherts: an early Devonian ecosystem preserved by hydrothermal activity. Pp. 131–149 *in* G. R. Brock & J. A. Goode (eds) *Evolution of Hydrothermal Ecosystems on Earth (and Mars?)*. John Wiley, Chichester.

— 2001. The Rhynie chert. Pp. 342–346 *in* D. E. G. Briggs & P. R. Crowther (eds) *Palaeobiology II*. Blackwell Scientific, London.

— **& Rice, C. M.** 1992. Stratigraphy and sedimentology of the Devonian Rhynie chert locality. *Scottish Journal of Geology* **28**: 37–47.

— **& Wilson, E.** 2004. Correlation of the Early Devonian Rhynie chert beds between three boreholes at Rhynie, Aberdeenshire, Scotland. *Scottish Journal of Geology* **40**: 73–81.

—, **Fayers, S. R. & Kelman, R.** 2003. Subaqueous silicification of the contents of small ponds in an Early Devonian hot spring complex, Rhynie, Scotland, *Canadian Journal of Earth Sciences* **40**: 1697–1712.